

Lasers in Manufacturing Conference 2021

Optical coherence tomography for 3D weld seam localization in absorber-free laser transmission welding

Frederik Maiwald^{a,*}, Clemens Roider^b, Michael Schmidt^{b,c}, Stefan Hierl^a

^aLabor Lasermaterialbearbeitung, Ostbayerische Technische Hochschule Regensburg, Am Campus 1, 92331 Parsberg, Germany

^bInstitute of Photonic Technologies, Friedrich-Alexander-Universität Erlangen-Nürnberg, Konrad-Zuse-Straße 3/5, 91052 Erlangen, Germany

^cErlangen Graduate School in Advanced Optical Technologies (SAOT), Paul-Gordan-Str. 6, 91052 Erlangen, Germany

Abstract

Thulium fiber lasers emit in the intrinsic absorption spectrum of polymers and enable the welding of transparent parts without absorbent additives. Focusing with high NA provides large intensity gradients inside the workpiece, enabling selective fusing of the joining zone without affecting the surface. Therefore, absorber-free laser transmission welding is well suited to fulfil the high demands on quality and reliability in the manufacturing of optical and medical devices. However, monitoring the welding process is required, since seam size and position are crucial for quality.

The aim of this work is the volumetric acquisition of the weld seam's location and size using optical coherence tomography. Due to the change of the optical properties during melting, the seam can be distinguished from the base material. The results coincide with microscopic images of microtome sections and demonstrate that weld seam localization in polyamide 6 is possible with an accuracy better than a tenth of a millimeter.

Keywords: laser transmission welding; transparent polymers; optical coherence tomography; process monitoring;

1. Introduction

1.1. Absorber-free laser transmission welding

A large number of medical and optical devices are made of transparent polymers. The manufacturing of these devices has high demands on cleanliness, precision, visual appearance and reliability. Advantages of

* Corresponding author. Tel.: +49-9492-8384-108

E-mail address: frederik.maiwald@oth-regensburg.de

absorber-free laser transmission welding – contactless input of energy, high precision, no adhesives and no particle formation – can be fully exploited for these applications (Polster 2009). Figure 1 shows the process principle of absorber-free laser transmission welding. Both joining partners are clamped in overlap. A laser beam with the wavelength in the polymers' intrinsic absorption spectrum between $1.6\ \mu\text{m}$ and $2\ \mu\text{m}$ is focused slightly below the joining zone. Focusing the beam with a comparably high numerical aperture (NA) provides large intensity gradients inside the specimen, enabling selective fusing of the joining zone. Thus, for example, the joining of two 1 mm thick partners with a 0.05 mm to 0.6 mm wide weld seam is possible without affecting the surface of the upper joining partner (Maiwald, Englmaier & Hierl 2020; Nguyen et al. 2020).

The main challenge in absorber-free welding is the exact generation of the weld seam in horizontal and vertical direction along the desired trajectory. The vertical expansion of the seam is crucial, since a molten surface leads to visible and palpable irregularities, whereas a too small seam causes instability and inadequate tightness (Mamuschkin et al. 2017; Nam-Phong et al. 2019; Polster 2009). In the manufacturing of medical fluidic devices, horizontal alignment is critical as well. If a fluidic channel is not sealed exactly at its edge, cells or drugs can temporarily linger and lump in remaining gaps, causing an unacceptable risk to the patient.

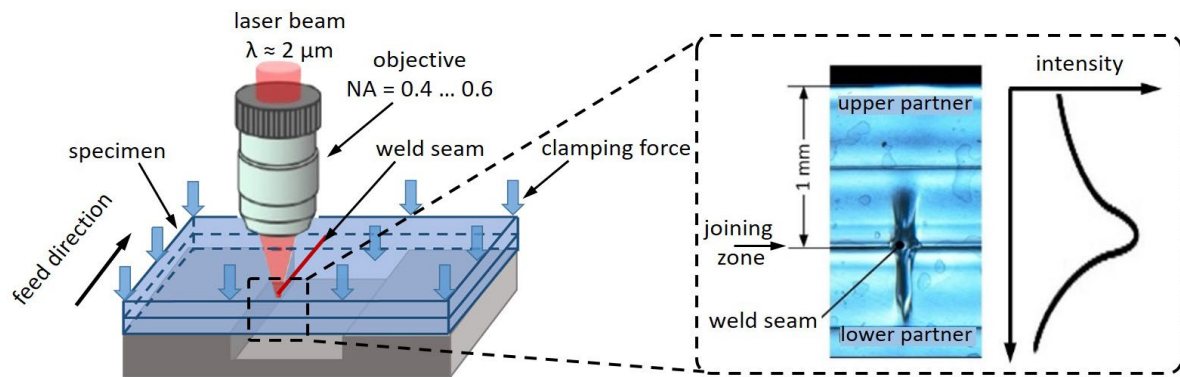


Fig. 1. Sketch of the experimental setup for absorber-free laser transmission welding (left) and an exemplary weld seam photographed in polarized light.

1.2. Process evaluation and monitoring

In addition to tests of the complete product such as burst pressure, leakage and drop-down tests, the weld seam must be separately analyzed to be able to validate the welding process itself. Conventionally, thin sections of the weld seam area are prepared by grinding or cutting with a microtome. The sections are viewed in polarized light in a transmitted light microscope. Due to the change of optical properties like birefringence during melting, the weld seam becomes visible (see fig. 1, right). However, only two-dimensional information, integrated along the thickness of the prepared thin-cut, is obtained. The three-dimensional examination of the parts is possible via computer tomography, enabling the detection of geometric errors like gaps, bubbles and melt blowouts based on the density change between the material and the air. However, the density difference of the base and the weld seam material is too small for detection via computer tomography.

Although the before-mentioned methods are already established, they have the significant disadvantage of being only applicable after processing where errors have already occurred. In contrast, inline (in-situ) process monitoring enables the direct observation during processing. Therefore, deviations can be identified live and compensated if necessary. In absorber-free laser transmission welding, pyrometer-based temperature monitoring can prevent overheating in corners and bubble formation, enabling a closed-loop control (Mamuschkin et al. 2017). Furthermore, the temperature signal is linked to the vertical expansion of the weld

seam, enabling indirect weld seam localization and adjustment of the vertical laser focus position (Maiwald, Englmaier & Hierl 2021; Mamuschkin et al. 2017). However, the effects of misplacement of the seam and incorrect temperature cannot be clearly distinguished from one another as no direct information about the geometry is determined.

In conclusion, the weld seam localization is crucial for quality, but the process stability and the possibilities to control this parameter are still insufficient. Therefore, the application of the absorber-free laser transmission welding process in the medical industry is still limited. We aim to improve this issue, by introducing optical coherence tomography into the process.

2. Optical coherence tomography

Optical coherence tomography (OCT) is an imaging technique capable of capturing volumetric images by analysing the reflections from surfaces and scattered light within the sample (Ruikang, Tuchin 2004). Figure 2 shows the setup used in this work, where a spectral domain OCT (SD-OCT) is attached to a 2D scanner. The low coherent light emitted by a super luminescent diode is divided into a sample and a reference path of an interferometer setup. The reflected light from the sample is collected and coupled back into the fibre. It is combined with the light of the reference arm and the resulting interferogram is measured by a spectrometer. The frequency of the interferogram is related to the depth locations in the sample. Therefore, the depth-reflectivity profile $R(z)$ can be extracted by a Fourier transform of the detected interferogram (Hitzenberger 2004). By scanning in two directions, the one-dimensional data is expanded volumetrically and a three-dimensional reflectivity profile $R(x, y, z)$ is obtained.

The OCT has excellent prerequisites for the online monitoring of laser-based processes. On the one hand, data points can be acquired with several hundred kHz, on the other hand, a scanner is already there. In conventional transparent-absorbent laser transmission welding, the OCT has already been used for process monitoring, enabling the detection of residual gaps, internal pores and the seam width (Schmitt et al. 2014). In these applications, there is always a clear boundary from plastic to air or combustion gases, leading to strong reflections due to the change of optical properties. However, in the case of absorber-free laser transmission welding studied in this work, transitions within the polymer - from the injection moulded base material to regions re-melted during welding - have to be resolved.

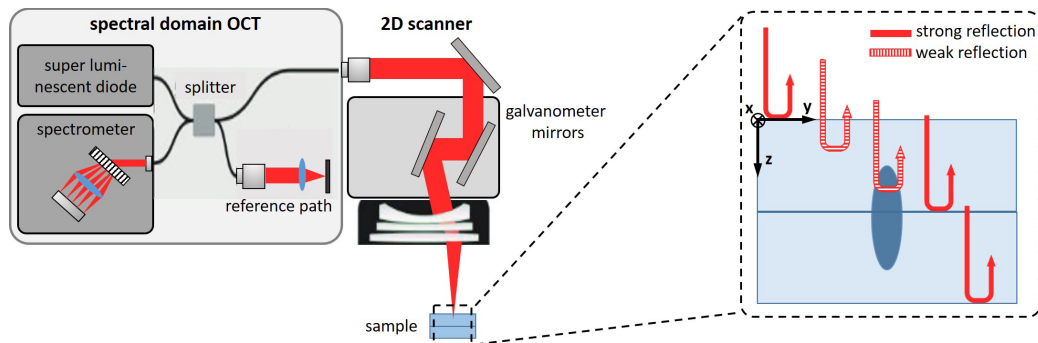


Fig. 2. Concept sketch of the scanner integrated OCT for volumetric weld seam analysis.

3. Experimental weld seam localization

3.1. Experimental Setup

For welding, a thulium fibre laser ($\lambda = 1940$ nm) with 120 W (cw) power is used. Figure 1 shows the experimental setup. The fixed-focus objective with a comparably high NA of 0.4 to 0.6 is mounted on an optical rail with slides. A fine threaded spindle moves the rail, enabling the variation of the distance between the optics and the specimen. A measurement system with a 0.01 mm resolution controls the rail's position. A clamping device with a conical slit hole fixes the two specimens ($50 \times 15 \times 2$ mm³ each) in overlap. It is moved by a 2-axis linear system enabling feed rates of up to 300 mm/s. The samples are made of semi-crystalline polyamide 6 (Ultramid B3s). We have already presented a detailed description of the experimental setup, the processing parameters and the simulation-based process layout (Maiwald, Englmaier & Hierl 2020).

For post-process weld seam analysis with OCT, a Telesto II OCT (Thorlabs) with the ThorImage 5.3.1.0 software and a central wavelength of 1.3 μ m is used for measurements with a 76 kHz acquisition rate. The measurement duration for a volume of $0.7 \times 3.7 \times 2.4$ mm³ (x, y, z), consisting of $256 \times 1536 \times 1024$ data points, is 16.5 seconds. This corresponds to an acquisition rate of 0.37 mm³ per second at a pixel size of 2.5 μ m. The refractive index of the base material is assumed to be 1.5.

3.2. Data acquisition and image processing

Figure 3 (a) shows an example of a volumetric view of the recorded data in the ThorImage OCT software. After the acquisition, the YZ slices are exported from ThorImage as 32-bit floating-point TIFF images without any processing (see Fig. 3 (b)). The subsequent image processing is performed automatically using self-written scripts in the free-to-use image processing software ImageJ. Figure 3 (c) shows a processed YZ slice. During image processing, the margins of the upper and the lower joining partner and the joining zone between both partners are determined first. Secondly, the weld seam is identified. Both steps are performed with separate scripts. Details of the image processing are explained below.

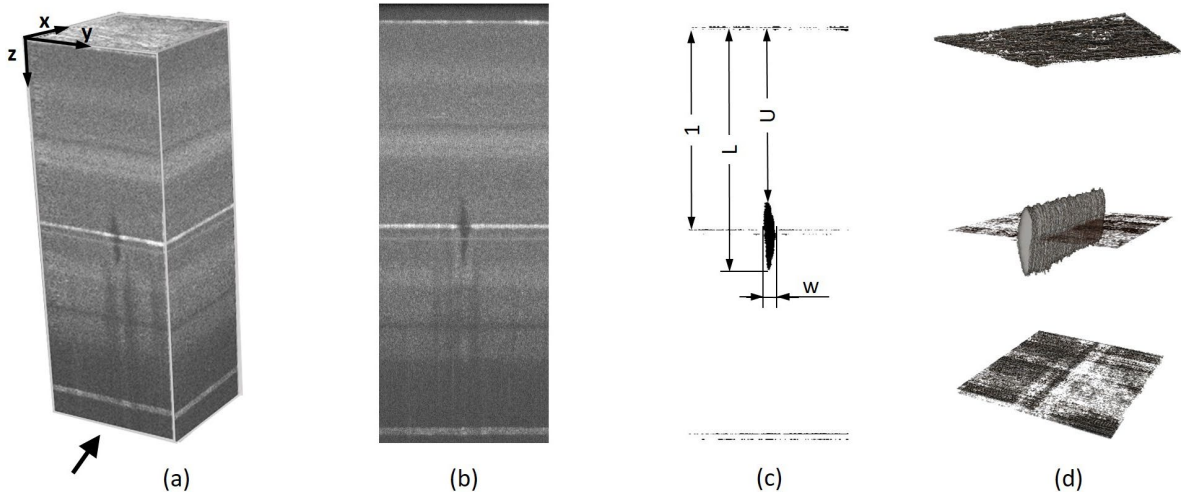


Fig. 3. (a) Volumetric view of the unprocessed data; (b) YZ slice of the volumetric data; (c) Processed image of the slice with the weld seam measurements; (d) Volumetric view of the processed data. The view shows the margins of the joining partners, the joining zone in the middle and the adjacent weld seam. Base area: 0.7×0.7 mm². Material: Ultramid B3S. Processing parameters: Rayleigh length = 0.3 mm, $\lambda = 1940$ nm, $\alpha = 0.83$ 1/mm, $v = 200$ mm/s, $E = 0.22$ J/mm.

The margins of both joining partners can be determined by simple thresholding since they are already clearly visible as bright lines in the raw data. Thus, the image is converted to binary, whereas grayscale values between 230 and 255 are set to white (255) and all others are set to black (0). After removing noise using the remove outliers function, the remaining binary image contains the margins of both joining partners and the data is transferred as CSV to MATLAB.

To determine the area of the weld seam, the unprocessed images are imported to ImageJ where the contrast is enhanced and the histogram is equalized before the image is converted to binary as well. In contrast to the previously mentioned identification of the margins, the “*isodata*”-algorithm is used for thresholding (Ridler & Calvard 1978). Since the weld seam does not clearly differ from the surrounding bulk material, several regions, which could potentially be the weld seam, remain in the YZ slices. To refine the selection, the blockwise “*remove outliers*” function is utilized, where the horizontal (y) and the vertical (z) size of the rectangle used for filtering can be defined. This makes use of the fact that in an YZ slice, the longer axis of the weld seam is vertical (z -direction), enabling the distinction from horizontally (y -direction) aligned features caused for example by the melt flow during injection moulding. After using the “*find connected regions*”-algorithm, which detects areas larger than 0.015 mm^2 , the remaining areas are exported to MATLAB and evaluated based on their location. Since the seam must be adjacent to the joining zone, it is checked if the images contain areas within 0.15 mm distance above or below the joining zone. The area is considered a seam if this query is true.

Finally, the seam width w and the distances between the upper surface and the upper (U) and lower (L) end of the weld seam are measured. The image is added to a three-dimensional array and the next image is processed. Figure 3 (d) shows the result after processing all images.

3.3. Experimental verification

Using the OCT, one weld seam per energy per unit length was measured in at least 250 YZ slices. To verify the weld seam measurements obtained via OCT, the results from the image processing are compared with reference data determined using microtome sections. For this, approximately $50 \text{ }\mu\text{m}$ thick cross-sections of at least seven welds per energy per unit length were prepared using a rotary microtome (Leica RM2255) as already presented in previous work (Maiwald, Englmaier & Hierl 2020). The sections were photographed in polarized light using a transmitted light microscope (Olympus BX53M). Afterwards, the weld seam areas are measured by hand using the image processing software ImageJ and OLYMPUS Stream Essentials Version 2.3. Figure 4 shows the distance between the specimen’s surface and the upper U and lower L end of the seam (a) as well as the seam width w (b) in dependence on the energy per unit length used for welding.

The seam’s height (L minus U) increases from 0.21 mm to 0.60 mm with increasing energy per unit length. Both the OCT data and the values obtained with thin cuts coincide well. Analysing the cuts, the seam width w increases from 0.05 mm to 0.11 mm with increasing energy per unit length. Analysing the OCT data, the seam width w is usually larger. At 0.32 J/mm and 0.35 J/mm , the seam width determined via OCT is twice the one by the manual method. This is due to the fact, that the melt is squeezed into the gap between the joining partners at this point. The melt blowout was only evaluated as part of the weld seam in the OCT, but not in the manual thin cut measurement. However, this difference in the evaluation method could be eliminated by a subsequent filtering of the OCT data if required.

The smallest (0.16 J/mm) and the largest (0.38 J/mm) weld seams would require other thresholds for OCT image processing. Therefore, the OCT data of these weld seams is missing in figure 4.

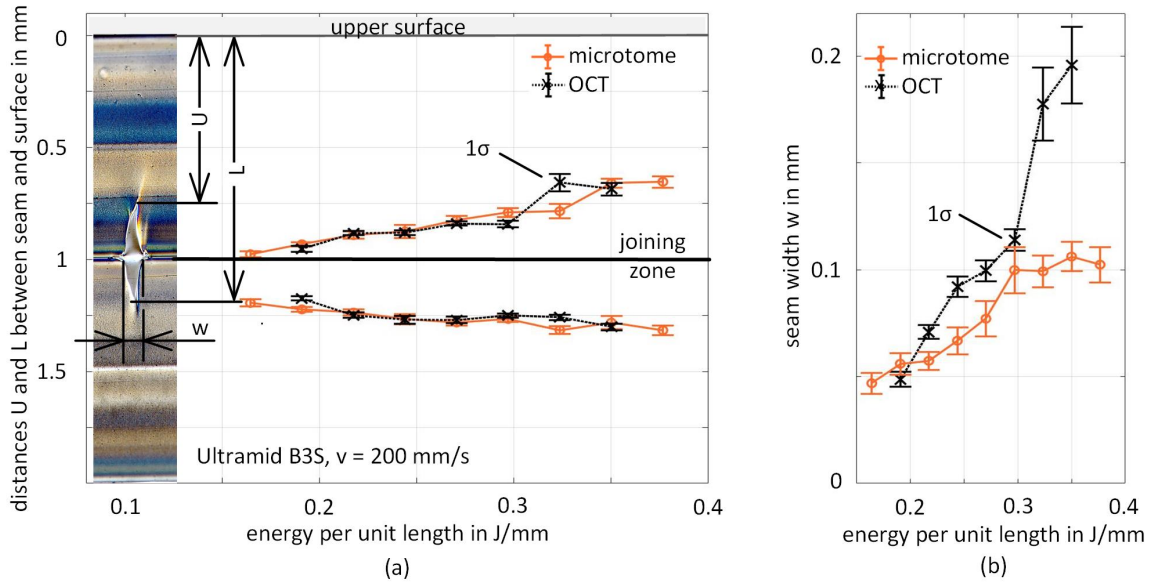


Fig. 4. (a) Distance between specimen's surface and upper (U) and lower (L) end of the seam as well as seam width w (b) in dependence on energy per unit length at 200 mm/s feed rate. Material: Ultramid B3S. Rayleigh length = 0.3 mm, $\lambda = 1940$ nm, $\alpha = 0.83$ 1/mm.

4. Conclusion and outlook

To fulfil the high demands on quality in the medical industry, we showed that optical coherence tomography can be used for three-dimensional weld seam localization. The results coincide well with the data determined manually by microtome cuts and subsequent polarized light microscopy, qualifying the OCT for quality assurance in absorber-free laser transmission welding. The method enables the automatized, three-dimensional evaluation of the weld seam size and position inside the volume of welded samples. Due to the OCT's excellent suitability for online process monitoring, live measurements during the welding process and studies with other materials are scheduled.

Acknowledgements

The authors gratefully thank the Bavarian Ministry for Economic Affairs, Media, Energy and Technology for funding the project "GipoWELD" and the project partner Arges for the good teamwork. Thanks to Gerresheimer Regensburg GmbH for providing samples and to Futonics Laser GmbH for providing a laser. We personally thank J. Tröger and E. Escher for their creative and helpful advice regarding OCT and image processing as well as A. Dzafic for language editing and proofreading.

References

- Hitzenberger, C.K., 2004, Absorption and Dispersion in OCT, In: Tuchin, V.V., Handbook of coherent domain optical methods: Biomedical diagnostics, environmental and material science, Kluwer Academic, Boston, p.138-142, ISBN: 1-4020-7885-4.
- Maiwald, F, Englmaier, S., Hierl, S., 2020, Absorber-free laser transmission welding of transparent polymers using fixed focus optics and 3D laser scanner, Procedia CIRP, vol. 94, pp. 686–90, doi: 10.1016/j.procir.2020.09.117.

- Maiwald, F, Englmaier, S., Hierl, S., 2020, 2021, Online Pyrometry for Weld Seam Localization in Absorber-Free Laser Transmission Welding of Transparent Polymers, *Journal of Micro / Nanoengineering*, vol. 16, no. 1, doi: 10.2961/jlmn.2021.01.2002.
- Mamuschkin, V, Haeusler, A, Engelmann, C, Olowinsky, A., Aehling, H., 2017, Enabling pyrometry in absorber-free laser transmission welding through pulsed irradiation, *Journal of Laser Applications*, vol. 29, no. 2, p. 22409, doi: 10.2351/1.4983515.
- Nam-Phong, N, Brosda, M, Olowinsky, A., Gillner, A., 2019, Absorber-Free Quasi-Simultaneous Laser Welding For Microfluidic Applications, *Journal of Laser Micro/Nanoengineering*, vol. 14, no. 3, 255-261, doi: 10.2961/jlmn.2019.03.0009.
- Nguyen, N-P, Behrens, S, Brosda, M, Olowinsky, A & Gillner, A., 2020, Laser transmission welding of absorber-free semi-crystalline polypropylene by using a quasi-simultaneous irradiation strategy, *Welding in the World*, vol. 64, no. 7, pp. 1227–35, doi: 10.1007/s40194-020-00913-3.
- Polster, S., 2009, Laserdurchstrahlschweissen transparenter Polymerbauteile, In: Geiger M., Feldmann. K., *Fertigungstechnik - Erlangen*, vol. 206, Meisenbach, Bamberg. pp. 8-9, doi: 10.25593/978-3-87525-294-1.
- Ridler, T.W., Calvard, S., 1978, Picture Thresholding Using an Iterative Selection Method, *IEEE Transactions on Systems, Man, and Cybernetics*, vol. 8, no. 8, pp. 630–2, doi: 10.1109/TSMC.1978.4310039.
- Ruikang, K.W, Tuchin, V.V., 2004, Optical Coherence Tomography, In: Tuchin, V.V., *Handbook of coherent domain optical methods: Biomedical diagnostics, environmental and material science*, Kluwer Academic, Boston, pp. 3-13, ISBN: 1-4020-7885-4.
- Schmitt, R, Mallmann, G, Devrient, M., Schmidt, M., 2014, 3D Polymer Weld Seam Characterization Based on Optical Coherence Tomography for Laser Transmission Welding Applications, *Physics Procedia*, vol. 56, pp. 1305–14, doi: 10.1016/j.phpro.2014.08.055.